have to verify the patient setup during the radiation treatment by subjective visual comparison between a portal image and a digitally reconstructed radiograph (DRR) produced in treatment planning, without any objective data on the setup errors, which are estimated by an independent method. In addition, even in facilities that have an automatic setup system, the patient setup error correction function does not always work well in an actual clinical setting, and thus a manual setup is often carried out after the automatic one. In such cases, experienced radiation oncologists can make a reproducible correction of the patient setup errors within a short period of time, but less experienced oncologists may not achieve the same performance. To resolve this issue, we here developed a computer-assisted radiotherapy system that can provide radiation oncologists with the objective data that are needed for correcting patient setup errors.

Many automated or semi-automated methods for estimation of patient setup errors have been studied based on two-dimensional (2D) or three-dimensional (3D) registration [3–10]. There are two types of patient setup methods based on registrations between two types of images, that is, 2D/2D and 3D/3D registrations. For 2D/2D registration, the 2D portal image and the 2D DRR image derived from a planning kV-3D computed tomography (CT) image or pre-treatment kV- or MV-3D CT image can be used [4, 5, 7, 8]. On the other hand, in 3D/3D registration, the planning kV-3D CT image can be registered with the pre-treatment kV- or MV-3D CT image [3, 6–10]. In conventional methods, the patient setups are performed by using registrations based on whole images including bony anatomical structures and soft tissue around the prostate. However, the displacements of the prostate and its surrounding anatomical structures could be independent of each other [11]. For that reason, radiation oncologists are likely to choose the localized anatomical structures closer to the prostate as reference points for estimation of setup errors. In addition, Morishita *et al.* [12] reported that localized anatomical templates that included the thoracic field, cardiac shadows, the superior mediastinum, lung apices, a part of the right lung and the right lower lung were useful for patient recognition in the picture archiving and communication system (PACS) environment. Therefore, based on the habits of radiation oncologists during clinical setup and the results of Morishita *et al.*, we considered that localized anatomical templates extracted from pelvic regions close to the prostate in the DRR image could feasibly be used for identifying the irradiation center in the portal image; these templates have not previously been studied for the estimation of patient setup errors. The purpose of this study was to develop a computerized method for estimating patient setup errors in portal images based on localized pelvic templates, including a clinical target volume for prostate cancer radiotherapy.

MATERIALS AND METHODS

Figure 1 shows an illustration of the overall scheme of the proposed method for estimation of patient setup errors in portal images, which mainly consisted of the following four steps.

(i) determination of an actual center of an irradiation field in the portal image;
(ii) extraction of a localized pelvic template with a prostate region of each patient using a mean pelvic template and four anatomical feature templates;
(iii) detection of a planned center in the portal image based on a technique for matching the portal image with the localized pelvic template;
(iv) estimation of the patient setup error by calculating the difference between the actual and planned centers in the portal image.

Clinical cases

This study was performed under a protocol approved by the institutional review board of the Kyushu University hospital. A training data set of 11 patients (ages: 60–84 years; median: 71 years) with prostate cancer, who received CRT through 2009, was selected for development of the proposed method. A total dose of 72 Gy in 36 fractions (2 Gy per fraction) was delivered for all patients during the

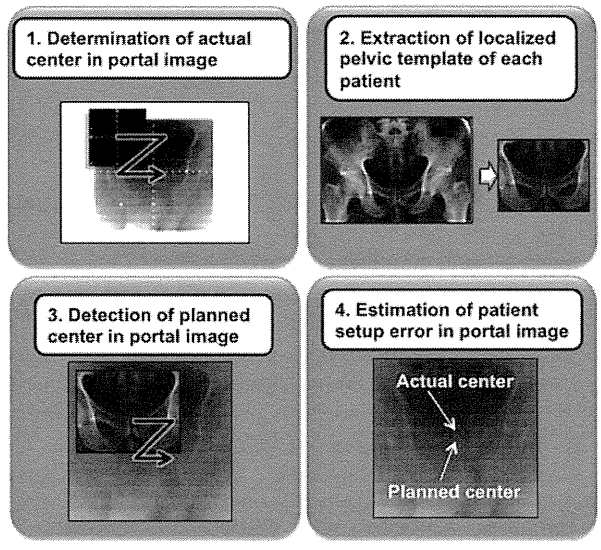

Fig. 1. An illustration of the overall scheme of our proposed method for estimating patient setup error in a portal image based on a localized pelvic template of an individual patient undergoing prostate cancer radiotherapy. The patient setup error was estimated by calculating the difference between the actual and planned centers in the portal image.

treatment course. The planning 3D CT images and the portal images for the 11 patients were used for development of the proposed method. All patients were scanned to acquire planning CT images using a four-slice CT scanner (Mx 8000; Philips, Einthoven, NL) with a slice thickness of 3.0 mm. The pixel sizes of the planning CT images were 0.78 mm ($n=2$), 0.82 mm ($n=1$), 0.86 mm ($n=2$), 0.88 mm ($n=4$) and 0.98 mm ($n=2$). The radiation treatment protocols were performed on an Eclipse treatment planning system (Varian Medical Systems Inc., Palo Alto, CA, USA). The portal images (matrix size: 512×384; pixel size: 0.56 mm; stored bits: 16) used for verification of patient setup prior to actual radiation delivery were acquired using 4- or 6-MV X-ray beams with a linear accelerator (Clinac 21 EX; Varian Medical Systems Inc.) that was equipped with an electronic portal imaging device (EPID) (AS-500; Varian Medical Systems Inc.). We selected eight portal images of eight patients at the last treatment time, and six portal images of three patients at two treatment times including the last one. The source-to-axis distance (SAD) and source-to-image receptor distance (SID) were 100 cm and 140 cm, respectively. Orthogonal portal images in the anterior–posterior (AP) (0°) and lateral projections (270°) were obtained to compare them with the corresponding planning DRRs.

A test data set of 10 prostate patients (ages: 64–79 years; median: 74.5 years) was selected for a validation test of the proposed method. There was no statistically significant difference in age between the training and test groups ($P=0.48$). The pixel sizes of the test planning CT images were 0.78 mm ($n=2$), 0.88 mm ($n=6$), 0.98 mm ($n=1$) and 0.90 mm ($n=1$).

Reconstruction of DRR images from planning CT images

The DRR images in the AP and lateral views were reconstructed as two beam's eye views from a 3D planning CT image in a world coordinate system including a linear accelerator and a planning CT image. The SAD and SID were 100 cm and 140 cm, respectively, which was the same geometry as for the EPID mounted on the linear accelerator. The isocenter in the planning CT image was placed at an SAD of 100 cm in the world coordinate system. The isocenter coordinate was obtained in a file of digital imaging and communications in medicine (DICOM) for radiation therapy, that is, a DICOM-RT file. Figure 2 shows an illustration of the reconstruction of a digitally reconstructed radiography (DRR) image from a planning CT image based on a ray casting method [13], where sampling points are obtained on a ray. For reconstruction of the DRR image, a divergent primary beam with a number of rays produced from an X-ray focal spot of the linear accelerator was virtually delivered to a 3D CT image. Then, CT values on each ray in the divergent beam in the 3D CT image were

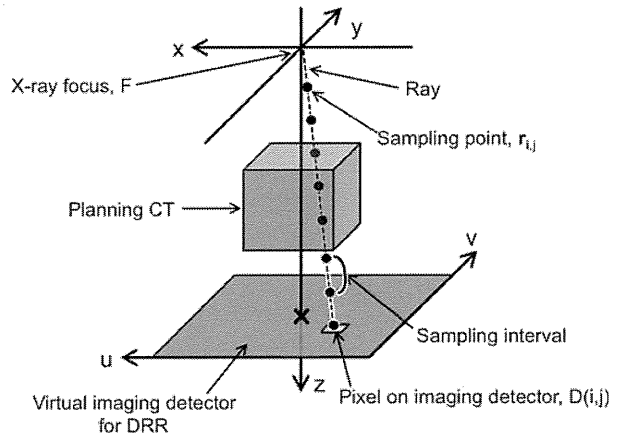

Fig. 2. An illustration of the reconstruction of a digitally reconstructed radiography (DRR) image from a planning CT image based on a ray casting method [13], where sampling points are obtained on a ray.

sampled at a certain interval and accumulated for each pixel in a virtual imaging plane, which had the same pixel size as the EPID (0.56 mm), but a 512×512 matrix size. The DRR image was reconstructed by the following equation:

$$D(i,j)=\sum_{n=1}^{N(i,j)} f\left(\mathbf{r}_n(i,j)\right) \tag{1}$$

where $D(i, j)$ is the pixel value on a virtual imaging detector for production of the DRR image, f is the planning CT image, $\mathbf{r}_n(i, j)$ is the nth sampling position vector on a ray from a pixel, $P(i, j)$, on the imaging detector to an X-ray focus, F, which was used for sampling CT values, and $N(i, j)$ is the number of the sampling data points for a pixel (i, j). The CT values on the ray were interpolated by using a cubic interpolation technique, because the coordinate of the sampling position on the ray was not always an integer but was always a real number.

Production of a mean pelvic template and anatomical feature templates

A localized pelvic template including a prostate region, which was used for detection of a planned center in the portal image, was extracted from the DRR image for each patient using a mean pelvic template and the four anatomical feature templates described below. A mean pelvic template image was produced from five training DRR images by registering all cases to one reference case by using an affine transformation with the anatomical feature points. Five training images with a typical bony pelvis in terms of size and shape were manually selected for producing the mean pelvic template image from the 11 training images used in this study, because the anatomical feature points used for production of localized pelvic templates were not accurately detected by the mean pelvic template and anatomical feature templates including atypical cases.

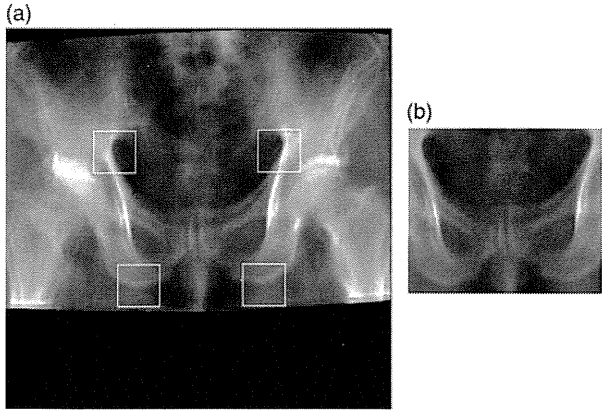

Fig. 3. (**a**) A mean DRR image in the anterior-posterior view, and (**b**) a mean pelvic template image. The white lines in Fig. 3a indicate four anatomical feature template regions.

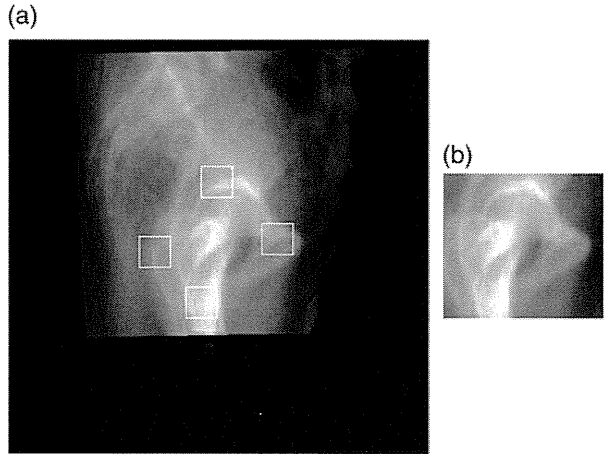

Fig. 4. (**a**) A mean DRR image in the lateral view, and (**b**) a mean pelvic template image. The white lines in Fig. 4a indicate four anatomical feature template regions.

In the clinical setting, the patient setup is usually performed based on anatomical characteristic bony structures around the prostate. Because the difference in movement between the prostate and the more distant bony structures can be large, radiation oncologists tend to select the localized bony structures closer to the prostate as anatomical feature points for estimating patient setup errors. Therefore, we manually selected the left and right lower ends of the ischial bone, and left and right ends of the foramen ischiadicum majora as four anatomical feature points in the AP view of the DRR image for the registration. The rectangular region, which was determined by the four feature points, included a prostate region. On the other hand, the four feature points in the lateral view were the apex of the symphysis pubis, acetabular upper end, inferior pubic ramus and back side of the upper end of the femur in the lateral view. Finally, the pelvic region in the mean DRR image was cropped as mean pelvic templates so that the four anatomical feature points could be included. Figure 3a and b shows a mean DRR image in the AP view, and a mean pelvic template image extracted from the mean DRR image, respectively, and Figure 4a and b show those in the lateral view.

Four anatomical feature templates of the corresponding anatomical regions mentioned above were extracted by a certain square region from the mean pelvic DRR images in the AP and lateral views, respectively. The template matrix size was empirically determined as 23 mm × 23 mm (41 × 41) pixels in this study. Figures 3a and 4a also show four regions (white lines) corresponding to the anatomical feature templates.

Estimation of the patient setup error

Determination of the actual center of an irradiation field in a portal image

The actual center in an irradiation field on the portal image was determined by searching a measuring scale within the irradiation field in the portal image using a template-matching technique based on the cross-correlation coefficient (CC). However, determination of the actual center of an irradiation field in a portal image depends on the individual institution, the imaging system used and whether or not the system includes an EPID. For example, the actual centers of the irradiation field in the portal image were determined by using hardware such as a measuring scale in some systems, including the system at our institution, but in other systems, the actual centers are identified using software. Therefore, the details of the method used to determine the actual center in an irradiation field on the portal image are described in Appendix A, because the method has not yet been standardized.

Extraction of a localized pelvic template of each patient

A localized pelvic DRR template of each patient in AP or lateral view was automatically extracted from his own DRR image by cropping a rectangular region, which was determined by using the mean pelvic template and four anatomical feature points. First, the mean pelvic template was registered with a DRR image of each patient by using the template-matching technique while maximizing a CC. The template matching was carried out within a radius of 1.0 cm from the isocenter in the DRR image. Next, each anatomical feature template was registered with its corresponding similar anatomical region within a radius of 1.0 cm from the original position in the mean pelvic template. Then, the localized pelvic template was extracted as a rectangular region determined with the minimum and maximum coordinates of the centers of four anatomical feature templates. Figure 5a, b and c shows a DRR image of a patient, its corresponding Sobel-filtered image (green)

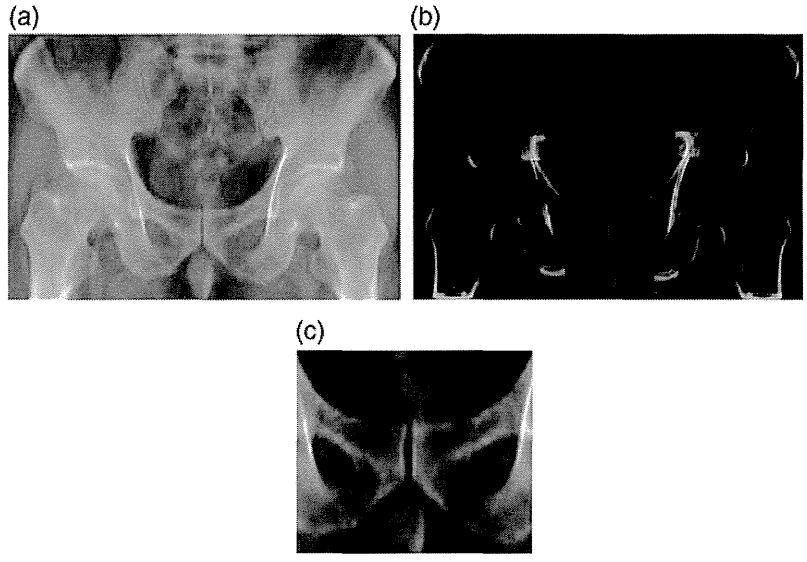

Fig. 5. (**a**) An original DRR image of a patient, (**b**) the corresponding Sobel-filtered image (green) with four feature regions (pink) detected by the anatomical feature templates and (**c**) a localized pelvic template of the same patient.

with four feature regions (pink) detected by the anatomical feature templates, and a localized pelvic template of the patient, respectively. Note that the size of the localized pelvic template shown in Fig. 5c is 80% of the size of the original pelvic template, which was automatically obtained from the patient's own DRR image by using the proposed method explained in this section. Because we investigated the effect of enhancement of bony anatomical structures on the overall performance of the proposed method, the localized pelvic template images with enhancement of bony structures by a Sobel filter were also produced for the estimation of patient setup errors.

Detection of the planned center in a portal image

The planned center in the irradiation field in a portal image was detected using the following two steps: (i) reduction of scale points on the portal image; and (ii) detection of the planned center based on a template-matching technique between the portal image and the localized pelvic template obtained as described in the previous section.

Although a measuring scale is needed to verify the center of the portal image and compare it with the planned isocenter of the planning DRR image in clinical practice, the measuring scale points should be reduced for more accurate template matching between the portal image and the localized pelvic template image. Therefore, the measuring scale points were reduced by inpainting each scale point with a mean filter and a measuring scale binary template. However, since the method seemed to be specific only when the measuring scale was used, the details of the method are illustrated in Appendix B.

The planned center in the irradiation field in the portal image was detected by performing a template matching between the localized pelvic template and the portal image. The planned center (x_{pc}, y_{pc}) of the irradiation field was determined by finding a location with the maximum similarity measure S (x, y) between the portal image I (x, y) and the template image T (x, y) based on the following equation:

$$(x_{pc}, y_{pc}) = \arg\max_{x,y}(S(x,y)). \quad (2)$$

In this template matching, we investigated the effects of the following three parameters on the performance of the proposed method: (i) the optimum size of the localized pelvic template; (ii) similarity measures, that is, the CC and mutual information (MI); and (iii) the enhancement of bony anatomical structures, which are described in 'Evaluation of the proposed method'.

Calculation of patient setup error

The patient setup error was estimated as the distance between the actual center and planned center in the irradiation field of the portal image in the AP, SI and (LR) directions and the 3D Euclidean distance.

Evaluation of the proposed method

The residual error [9] between the patient setup errors obtained by the proposed method and gold standard setup errors obtained by the radiation oncologists was calculated for evaluation of the proposed method. The gold standards for the setup errors were determined based on a consensus

between two experienced radiation oncologists in this study. However, note that we did not investigate the inter-observer variability and intra-observer variability of the gold standards of patient setup errors. The residual error denotes the differences between the patient setup errors obtained by the proposed method and the gold standard patient setup errors. Residual error was calculated in the AP, SI and LR directions and for the Euclidean distance. The residual error of the 3D Euclidean distance was employed for evaluation of the overall performance of the proposed method.

We applied the proposed method to the training data set of 11 prostate patients, that is, a resubstitution test, as well as to the test data set of 10 prostate patients, which was not used for development of the proposed method, that is, a validation test.

To find the optimum parameters for use in the proposed method, we investigated the effects of the following three parameters on the performance of the method: (i) the optimum size of the localized pelvic template; (ii) similarity measures, that is, the CC and MI; and (iii) the enhancement of bony anatomical structures.

Optimum size of the localized pelvic template

In a majority of image-guided radiotherapy systems, the patient setups are performed by using registrations based on whole anatomical structures including soft tissue around the prostate. However, since the prostate and its surrounding anatomical structures can displace independently of each other [11], radiation oncologists are likely to adopt the anatomical structures closer to the prostate (e.g. the pubic symphysis) as reference points. Therefore, the optimum size of the localized pelvic template was investigated by reducing the localized pelvic template size determined in the previous section from 100% to 40% relative size. We defined the 100% relative size for the localized pelvic template as the size of the original pelvic template, which was automatically obtained from the patient's own DRR image by using the method described in the previous section.

Similarity measures

In general, since the accuracy of the registration or template-matching technique in this study depends on the similarity measure, the detection accuracy of the planned center in the irradiation field may change with the similarity measure. In addition, according to a study of Wu *et al.* [14], the robust similarity measures in the patient setup using a registration technique were a normalized CC and normalized MI. Therefore, we evaluated the performance of the proposed method with two similarity measures, that is, the CC and MI, which are widely used for registration in radiological fields.

The CC between the portal image $I(x, y)$ and the template image $T(x, y)$ was based on the following equation [15, 16]:

$$C(x',y') = \frac{1}{X \cdot Y} \sum_{x=0}^{X-1} \sum_{y=0}^{Y-1} \frac{(I(x,y) - \bar{I})(T(x,y) - \bar{T})}{\sigma_i \cdot \sigma_t} \quad (3)$$

where x and y are the coordinates in the image within the overlapped area between the portal and template images, x' and y' are the center coordinates of the template image, $I(x, y)$ is the pixel value at (x, y) in the portal image, $T(x, y)$ is the pixel value at (x, y) in the template image, $\bar{I}$ and σ_i are the mean and the standard deviation of the pixel values of the portal image, respectively, $\bar{T}$ and σ_t are the mean and the standard deviation of the pixel values of the template image within the same overlapped area, respectively, and X and Y are the numbers of pixels in x and y widths of the template image, respectively.

The mutual information at the center coordinate (x', y') between the template image and the portal image was calculated from the following equation [17]:

$$M(x',y') = \sum_{a=0}^{L-1} \sum_{b=0}^{L-1} P_{it}(a,b) \log_2 \frac{P_n(a,b)}{P_i(a)P_t(b)} \quad (4)$$

$$P_{it}(a,b) = \frac{h(a,b)}{X \cdot Y} \quad (5)$$

$$P_i(a) = \sum_{b=0}^{L-1} P_{it}(a,b) \quad (6)$$

$$P_t(b) = \sum_{a=0}^{L-1} P_{it}(a,b) \quad (7)$$

where L is the number of quantization levels; $P_i(a)$ is the probability that the intensity at a pixel in the portal image is a; $P_t(b)$ is the probability that the intensity at a pixel in the template image is b; $P_{it}(a, b)$ is the joint probability that the intensity at a pixel in the portal image is a in conjunction with the event that the intensity at a pixel in the template image is b; $h(a, b)$ is the 2D histogram for the case that the intensity at a pixel in the portal image is a in conjunction with the event that the intensity at a pixel in the template image is b.

Enhancement of bony anatomical structures

In the current image-guided radiation therapy for prostate cancer, in general, the patient setup is performed based on the pelvic bony anatomical structures close to a target. Therefore, we investigated the effect of the enhancement of the bony structures in the pelvic DRR templates and portal images on the performance of the proposed method. Prior

to the investigation, we applied two famous edge enhancement filters, that is, the Sobel filter and Laplacian of Gaussian (LoG) [18]. As a result, the residual errors in the Euclidean distance for the Sobel filter and LoG were 2.65 $\pm$ 1.21 mm and 2.81 $\pm$ 1.2 mm, respectively, which indicated no statistically significant difference. However, it takes more time to apply the LoG filter compared with the Sobel filter. Consequently, the Sobel filter with the structure element of a 3×3 square was used for enhancement of the bony structures in this study. Kondo *et al.* [19] reported that their template matching technique with a Sobel filter was useful in preventing 'wrong' images from being stored in the correct location, for example, in the proper patient's folder in a PACS environment.

RESULTS

The actual centers in an irradiation field on the portal images were determined with high accuracy by the proposed method of searching a measuring scale using a template-matching technique. The average errors between actual centers derived from the proposed method and the gold standard actual centers were 0.3 ± 0.14 mm in Euclidean distance for the resubstitution test and 0.25 ± 0.31 mm for the validation test.

We determined the optimum size of the localized pelvic template image by investigating the effect of the template size on the residual error of the Euclidean distance in the patient setup errors. The proposed method was applied to 11 training cases. Figure 6 shows an example of localized pelvic templates for an AP and lateral views with a reduction of 100% to 40% relative size. Figure 7 shows the relationship between the relative size for the localized pelvic template image and the residual error in Euclidean distance obtained by the proposed method. The results showed that the optimum localized pelvic template size was 80% of the original localized template image that was used for estimation of the patient setup errors in this study.

Tables 1 and 2 show the residual errors for the training and test data sets, respectively, that is, the mean, SD and minimum and maximum values of residual error in the LR, SI and AP directions and for the Euclidean distance obtained by using the CC or MI, and with or without a Sobel filter. Each value was obtained by averaging the values for all cases. The proposed method using the CC with the Sobel filter achieved the minimum residual errors of 2.65 ± 1.21 mm and 3.10 ± 1.49 mm for the resubstitution and validation tests, respectively. The second minimum residual error was obtained by the method using the mutual information with the Sobel filter in both tests. Tables 3 and 4 show the P-values for statistical significance for the training and test data sets, respectively, in the residual error of the Euclidean distance between combinations of two similarity measures, that is, the CC and MI, with or without a Sobel filter. According to these results, the residual errors of the Euclidean distance by the two similarity measures with the Sobel filter were significantly smaller than those without the Sobel filter. In addition, there were no statistically significant differences in the residual errors of the Euclidean distance between the methods using the cross-correlation coefficient and mutual information with a Sobel filter ($P > 0.05$). Furthermore, there were no statistically significant differences in the residual errors in the three directions and the residual error for the Euclidean distance between the resubstitution and validation tests ($P > 0.05$).

The residual errors in the three directions (LR, SI and AP) obtained by the method using the CC with the Sobel filter were smaller than 2 mm in both tests, as shown in

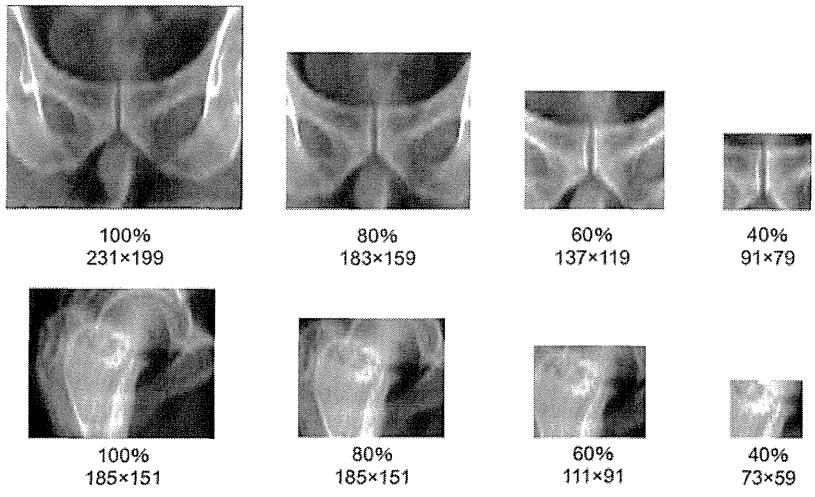

Fig. 6. An example of localized pelvic templates for an AP and lateral views with reductions of 100% to 40% relative size. The percent relative size and matrix size are shown under each template.

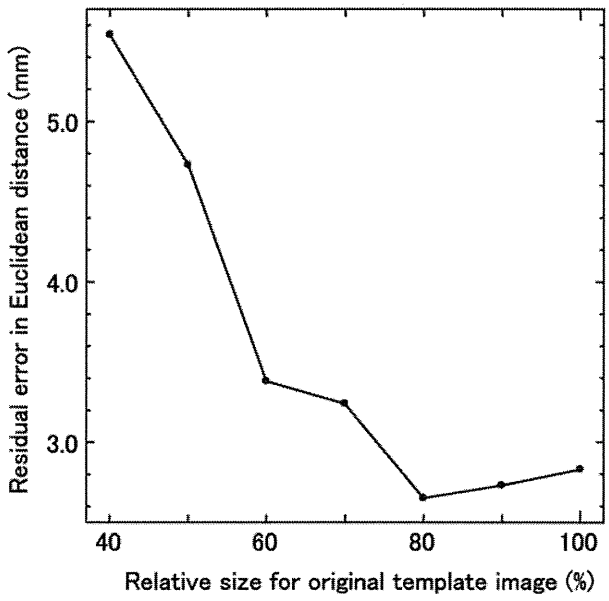

Fig. 7. Relationship between the relative size for the localized pelvic template image and the residual error in Euclidean distance obtained by the proposed method. Note that the 100% relative size for the localized pelvic template was the original pelvic template, which was automatically obtained from the patient's own DRR image by cropping a rectangular region.

Tables 1 and 2. These residual errors are smaller than a tolerance of 2 mm for imaging and treatment coordinate coincidence in the EPID, which is recommended by the American Association of Physicists in Medicine Task Group 142 [20]. Tables 5 and 6 show the *P*-values for statistical significance for the training and test data sets, respectively, in the residual error between the two directions using CC and MI with a Sobel filter. These results indicate that there were no statistically significant differences in the residual error between the two directions by either method or with either test ($P > 0.05$).

The average calculation time of patient setup errors by the proposed method was about 10 s on a personal computer with a 3.33-GHz central processing unit (Intel, Core (TM) 2 Duo) and 4.0-GB memory, excluding the production of AP and lateral DRR images, which required about 8 min on average to obtain the DRR images.

DISCUSSION

Although a number of papers have been published on the detection of patient setup errors, most of these papers have involved phantom studies rather than patient studies. We compare the proposed method with two past studies, in which the methods for detection of setup errors were applied to patient data as validation tests. Thilmann *et al.*

Table 1. The mean, SD and minimum and maximum values of residual error in the left–right, superior–inferior and anterior–posterior directions and residual error for the Euclidean distance obtained by using the cross-correlation coefficient or mutual information, with or without a Sobel filter, for a training data set

		Residual error (mm)			
Method	**Direction**	**Mean**	**SD**	**Min**	**Max**
CC	LR	1.17	0.98	0.00	4.20
	SI	1.44	1.23	0.00	4.48
	AP	6.60	3.59	1.12	11.53
	Euclidean	7.27	3.09	2.46	11.87
CC + Sobel	LR	1.33	0.93	0.56	4.20
	SI	1.28	0.98	0.00	2.80
	AP	1.58	0.86	0.00	2.81
	Euclidean	2.65	1.21	0.56	5.78
MI	LR	1.81	2.17	0.00	6.99
	SI	4.56	3.43	0.56	9.53
	AP	4.68	3.69	0.56	9.85
	Euclidean	8.25	2.84	3.23	13.43
MI + Sobel	LR	1.33	0.93	0.56	4.20
	SI	1.28	0.98	0.00	2.80
	AP	2.14	2.23	0.00	9.57
	Euclidean	3.13	2.23	0.56	9.84

LR = left–right; SI = superior–inferior; anterior–posterior = AP; CC = cross-correlation coefficient; MI = mutual information.

[6] developed a reliable workflow from image acquisition to correction of interfraction setup errors using kV cone beam CT (CBCT). In their method, the registration between the CBCT with the planning CT is achieved by using an automatic matching algorithm that maximizes mutual information. In their application of the automatic registration to two prostate cancer patients, the mean residual error was 3.2 mm. Wierzbicki *et al.* [10] proposed two fully automatic image-guided radiotherapy (IGRT) techniques, that is, 'forward' and 'reverse' IGRT techniques, based on a linac-integrated CBCT system that requires a significantly smaller imaging dose. When using the reverse technique, which involves non-rigid deformation of the planning CT and contours to match the CBCT, their image guidance method showed a mean residual error of 3.3 mm for prostate cancer in 10 patients while requiring only 20% of the standard imaging dose. On the other hand, our results showed that the mean residual error was 3.1 mm for the validation test with 10 cases, which seems to be comparable with past studies.

Table 2. The mean, SD and minimum and maximum values of residual error in the left–right, superior–inferior and anterior–posterior directions and residual error for the Euclidean distance obtained by using the cross-correlation coefficient or mutual information, with or without a Sobel filter, for a test data set

		Residual error (mm)			
Method	**Direction**	**Mean**	**SD**	**Min**	**Max**
CC	LR	1.25	1.13	0.00	3.24
	SI	1.72	1.41	0.00	4.80
	AP	3.97	3.12	0.56	9.60
	Euclidean	5.18	2.52	0.97	9.76
CC + Sobel	LR	1.20	1.12	0.00	3.24
	SI	1.50	1.51	0.00	4.24
	AP	1.72	1.29	0.00	4.25
	Euclidean	3.10	1.49	0.56	5.03
MI	LR	0.97	0.77	0.00	2.68
	SI	2.22	2.64	0.00	8.71
	AP	6.45	3.34	1.13	9.60
	Euclidean	7.46	3.25	2.29	12.93
MI + Sobel	LR	1.20	1.01	0.00	3.24
	SI	1.38	1.56	0.00	4.24
	AP	1.77	1.25	0.00	4.25
	Euclidean	3.12	1.33	1.12	4.69

See Table 1 note for abbreviations.

Table 3. Statistical significance (P-value) in the residual error of the Euclidean distance between combinations of two similarity measures, that is, cross-correlation coefficient (CC) and mutual information (MI), with or without a Sobel filter for a training data set

	CC	**CC + Sobel**	**MI**	**MI + Sobel**
CC		–	–	–
CC + Sobel	0.000032		–	–
MI	0.408930	0.000001		–
MI + Sobel	0.000584	0.497856	0.000026	

See Table 1 note for abbreviations.

Table 4. Statistical significance (P-value) in the residual error of the Euclidean distance between combinations of two similarity measures, that is, cross-correlation coefficient and mutual information, with or without a Sobel filter for a test data set

	CC	**CC + Sobel**	**MI**	**MI + Sobel**
CC		–	–	–
CC + Sobel	0.046963		–	–
MI	0.114838	0.001802		–
MI + Sobel	0.043631	0.976325	0.001615	

See Table 1 note for abbreviations.

Table 5. Statistical significance (P-value) in the residual error between two directions using cross-correlation and mutual information with a Sobel filter for a training data set

	LR–SI	**SI–AP**	**AP–LR**
CC + Sobel	0.894853	0.415737	0.484603
MI + Sobel	0.894853	0.212833	0.236069

See Table 1 note for abbreviations.

Table 6. Statistical significance (P-value) in the residual error between two directions using cross-correlation and mutual information with a Sobel filter for a test data set

	LR–SI	**SI–AP**	**AP–LR**
CC + Sobel	0.638753	0.741841	0.638753
MI + Sobel	0.764862	0.565630	0.764862

See Table 1 note for abbreviations.

In this preliminary study, the proposed method was focused on translation in the LR, SI and AP directions so that we could investigate the usefulness of the localized pelvic templates. Because the prostate is located in the middle of the patient body, the proposed method based on the localized pelvic templates including regions close to the prostate would not be influenced by the patient rotation around the LR, SI and AP axes. Nevertheless, the proposed method should be expanded to the 3D localized pelvic templates in order to account for the patient rotation.

We dealt with the estimation of setup errors of prostate cancer patients in this study. In principal, the proposed method may be applied to other cancers, such as head and neck cancers. However, for cancers in mobile parts of the patient body or cancer deformation, we should incorporate non-rigid registration techniques into the template-matching technique using localized templates.

The purpose of this study was to investigate the usefulness of the proposed method based on the localized pelvic templates for detection of patient setup errors. To investigate the usefulness, we applied a whole-pelvic-template-based method, which used a different template from the proposed method but the same algorithm, to the same 11 training cases as used for development of the proposed method. The results showed that the average residual errors of the patient setup error using the whole and localized pelvic templates were 2.61 and 1.33 mm in the LR

direction, 2.36 and 1.28 mm in the SI direction, 2.47 and 1.58 mm in the AP direction, and 5.12 and 2.56 mm in Euclidean distance, respectively. We believe that the proposed method based on the localized pelvic templates could be useful for the detection of patient setup errors.

In this paragraph, we discuss the results of investigation of the effects of the following three parameters on the performance of the proposed method: (i) optimum size of the localized pelvic template; (ii) similarity measures; and (iii) enhancement of bony anatomical structures.

Optimum size of the localized pelvic template

As shown in Fig. 6, the optimum localized pelvic template size was 80% of the original localized template image, which was used in the proposed method for estimation of the patient setup errors. The 80% templates included a sufficient characteristic region of the bone structures around the prostate, such as the ischial tuberosity and obturator foramen for the pelvic template matching. In contrast, the 100% templates sometimes also contained the outside regions of ischial tuberosity, whose appearance in the EPID portal image could vary when the patient rolled on the treatment table, due to their distance from the body axis. Therefore, the larger pelvic template may not work well for estimation of patient setup errors. On the other hand, templates smaller than 80% relative size may not contain a sufficient characteristic region of the bone structures, and thus such templates might not be useful for pelvic template matching.

Similarity measures

As shown in Tables 1 and 2, the method using the CC can more correctly detect the patient setup errors than the method using MI regardless of whether or not the Sobel filter is applied. The CC is considered to be the degree of similarity between two images with respect to the spatial distribution of pixel values, and it could be useful for two images with similar image quality. The MI is based on a two-dimensional pixel value histogram, and is intuitively regarded as the shared information between two images, which can be used as a degree of similarity. MI is considered to be useful for evaluation of the similarity between two images with different image quality, such as CT and positron emission tomography images. In this study, because both the DRR and EPID portal images are based on the degree of attenuation of X-rays for the human body, the spatial distributions of pixel values of the two images are similar to each other. Therefore, the method with the CC would be better to obtain the patient setup errors.

Enhancement of bony anatomical structures

The method with the Sobel filter was better for evaluating setup errors than that without the Sobel filter, irrespective of the similarity measure, as shown in Tables 1 and 2. The reason for this result was considered to be that the pelvic template matching using the DRR and EPID portal images depends on the bone structures, because soft tissue structures were hardly imaged in the DRR and EPID portal images. Therefore, the enhancement of bone structures was useful for the detection of patient setup errors.

Since the localized pelvic DRR template was extracted from the patient's own DRR image produced from his planning CT images, the localized templates could reflect the patient's clinical condition, such as the degree of obesity, weight and the degree of bladder filling when imaging the planning CT. However, the patient's clinical condition at imaging of the planning CT is not exactly the same as that at the treatment time, and the patient condition could vary during the course of treatment, since the treatment often consisted of around 36 fractions (e.g. many patients lost weight during the treatment). Consequently, the condition of bone structures could change, and the localized templates would not be optimum. Therefore, in a future work we should incorporate non-rigid registration techniques into the template-matching technique using the localized templates in consideration of the change in the patient's condition.

To further confirm its robustness, the proposed method should be applied to many test cases, since we performed a validation test using only 10 cases in this study. In addition, we should employ test cases including portal images and CT images, which could be acquired from different equipment in different institutions. We believe that the proposed method can be improved by performing such validation tests as a next step, such that the method will ultimately be able to detect patient setup errors with high accuracy for many different types of cases.

CONCLUSIONS

We have developed a computerized method for estimation of patient setup errors in portal images based on localized pelvic templates for prostate cancer radiotherapy. The patient setup errors were estimated based on a template-matching technique between the portal image and a localized pelvic template image around a clinical target volume for each patient. The residual errors in the three directions (LR, SI and AP) obtained by the method were <2 mm in both tests. There were no statistically significant differences in the residual error between the test for training cases and the validation test ($P = 0.438$). The proposed method appears to be robust for the detection of patient setup error at a treatment session.

ACKNOWLEDGEMENTS

This research was partially supported by a Research Grant, Academic Challenge, from The Robert T. Huang

Entrepreneurship Center of Kyushu University, and by a Grant-in-Aid for Scientific Research (C), 22611011, 2010, from the Ministry of Education, Culture, Sports Science, and Technology (MEXT).

APPENDIX A DETERMINATION OF THE ACTUAL CENTER OF AN IRRADIATION FIELD IN A PORTAL IMAGE

The actual center in an irradiation field on a portal image was determined by searching a measuring scale within the irradiation field in the portal image using a template matching technique based on the cross-correlation coefficient [15, 16]. A measuring scale was superimposed on the portal image for two clinical purposes: verification of the center of the portal image and comparison with the planned isocenter of the planning DRR image. Prior to this process, the irradiation field was extracted based on a pixel-value histogram analysis. First, the initial irradiation field in the portal image was roughly extracted by a threshold value, which was determined by subtraction of the SD of the largest peak in a portal image histogram from the pixel value of the corresponding largest peak [16]. Then, the final irradiation field was segmented by cropping a field 3-mm smaller than the circumscribed quadrangle of the initial irradiation field, because the near edge of the initial irradiation field was not segmented well. Figure A1a, b and c show a portal image with a measuring scale, an initial irradiation field and a final irradiation field, respectively.

The center of the measuring scale in the portal image was detected as an actual center of the irradiation field based on a template matching between the portal image and the standard scale point template. The actual center of the irradiation field was determined by finding a location with the maximum cross-correlation coefficient between the portal image and the template image. Figure A2 shows a standard measuring scale point template used for determination of the center of the irradiation field. This template was obtained from a portal image, which was acquired without any objects by mounting the measuring scale to a gantry head of the linear accelerator.

APPENDIX B REDUCTION OF SCALE POINTS IN THE PORTAL IMAGE

The measuring scale points should be reduced for more accurate template matching between the portal image and the localized pelvic template image. Therefore, the measuring scale points were reduced by inpainting each scale point with a mean filter and a measuring scale binary template. Figure A3 shows illustrations of the reduction of scale points in the portal image by inpainting the scale points with a mean filter. A measuring scale superimposed in an original portal image is shown in Figure A3a. To reduce the scale points in the portal image, the mean filter with the structure element of a circle (radius: nine pixels) was applied to each pixel within each circle scale point in the measuring scale binary template (Figure A3b), which was overlaid on the original portal image (Figure A3a) in the position of the actual center of the irradiation field. The mean value was calculated within the neighbor pixels in

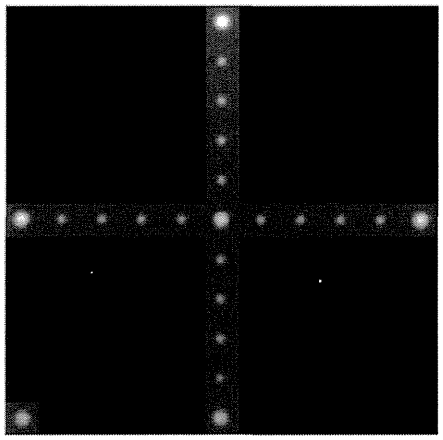

Fig. A2. Standard measuring scale point template image used for determination of the center of the irradiation field.

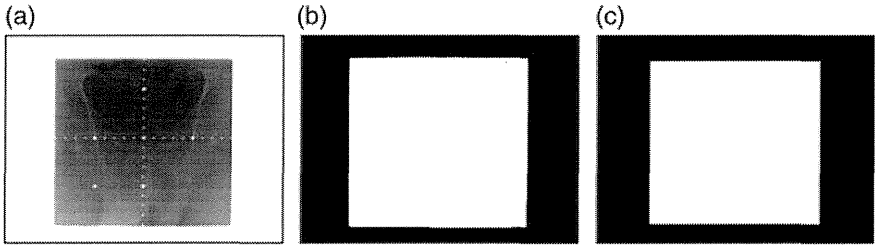

Fig. A1. Illustrations of (**a**) a portal image with a measuring scale, (**b**) an initial irradiation field and (**c**) a final irradiation field.

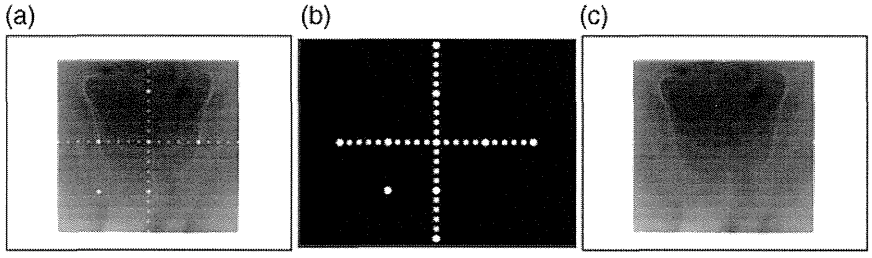

Fig. A3. Illustrations of the reduction of scale points in a portal image by inpainting of the scale points with a mean filter: (**a**) an original portal image, in which a measuring scale was superimposed, (**b**) a measuring scale binary template and (**c**) the portal image with reduced scale points.

the circle of the mean filter excluding the circle scale point region. Finally, a median filter with a 3×3 square structure element was used for removal of the very small amount of noise. Figure A3c shows the portal image with reduced scale points.

REFERENCES

1. Uchida T, Shoji S, Nakano M *et al.* High-intensity focused ultrasound as salvage therapy for patients with recurrent prostate cancer after external beam radiation, brachytherapy or proton therapy. *BJU Int* 2011;**107**(3):378–2.
2. Mangar SA, Huddart RA, Parker CC *et al.* Technological advances in radiotherapy for the treatment of localised prostate cancer. *Eur J Cancer* 2005;**41**(6):908–21.
3. Court LE, Dong L. Automatic registration of the prostate for computed-tomography-guided radiotherapy. *Med Phys* 2003;**30**(10):2750–7.
4. Matsopoulos GK, Asvestas PA, Delibasis KK *et al.* Registration of electronic portal images for patient set-up verification. *Phys Med Biol* 2004;**49**(14):3279–89.
5. Tanaka R, Matsushima M, Kikuchi Y *et al.* Development of computerized patient setup verification and correction system in radiotherapy. *Japanese Journal of Radiological Technology* 2005;**61**:1689–99.
6. Thilmann C, Nill S, Tücking T *et al.* Correction of patient positioning errors based on in-line cone beam CTs: clinical implementation and first experiences. *Radiat Oncol* 2006;**1**(16):1–9.
7. Ploquin N, Rangel A, Dunscombe P. Phantom evaluation of a commercially available three modality image guided radiation therapy system. *Med Phys* 2008;**35**(12):5303–11.
8. Wang Z, Nelson JW, Yoo S *et al.* Refinement of treatment setup and target localization accuracy using three-dimensional cone-beam computed tomography for stereotactic body radiotherapy. *Int J Radiat Oncol Biol Phys* 2009;**73**(2):571–7.
9. Kudchadker PJ, Lee AK, Yu ZH *et al.* Effectiveness of using fewer implanted fiducial markers for prostate target alignment. *Int J of Radiat Oncol Biol Phys* 2009;**74**(4):1283–9.
10. Wierzbicki M, Schaly B, Peters T *et al.* Automatic image guidance for prostate IMRT using low dose CBCT. *Med Phys* 2010;**37**(7):3677–86.
11. Schallenkamp JM, Herman MG, Kruse JJ *et al.* Prostate position relative to pelvic bony anatomy based on intraprostatic gold markers and electronic portal imaging. *Int J Radiat Oncol Biol Phys* 2005;**63**(3):800–11.
12. Morishita J, Katsuragawa S, Sasaki Y *et al.* Potential usefulness of biological fingerprints in chest radiographs for automated patient recognition and identification. *Acad Radiol* 2004;**11**(3):309–15.
13. Sherouse GW, Novins K, Chaney EL. Computation of digitally reconstructed radiographs for use in radiotherapy treatment design. *Int J Radiat Oncol Biol Phys* 1990;**18**(3):651–8.
14. Wu J, Kim M, Peters J *et al.* Evaluation of similarity measures for use in the intensity-based rigid 2D-3D registration for patient positioning in radiotherapy. *Med Phys* 2009;**36**(12):5391–403.
15. Arimura H, Katsuragawa S, Li Q *et al.* Development of a computerized method for identifying the posteroanterior and lateral views of chest radiographs by use of a template matching technique. *Med Phys* 2002;**29**(7):1556–61.
16. Arimura H, Egashira Y, Shioyama Y *et al.* Computerized method for estimation of the location of a lung tumor on EPID cine images without implanted markers in stereotactic body radiotherapy. *Physics in Medicine and Biology* 2009;**54**:665–77.
17. Ding L, Goshtasby A, Satter M. Volume image registration by template matching. *Image and Vision Computing* 2001;**19**(12):821–32.
18. Burger W, Burge MJ. *Digital Image Processing: an Algorithmic Introduction Using Java* 1st ed. New York: Springer, 2007.
19. Kondo K, Morishita J, Katsuragawa S *et al.* Development of an automated patient-recognition method for digital chest radiographs using edge-enhanced images. *Nippon Hoshasen Gijutsu Gakkai Zasshi* 2003;**59**(10):1277–84 (in Japanese).
20. Klein EE, Hanley J, Bayouth J *et al.* Task Group 142, American Association of Physicists in Medicine. Task Group 142 report: quality assurance of medical accelerators. *Med Phys* 2009;**36**(9):4197–212.

Int. J. Radiation Oncology Biol. Phys., Vol. 82, No. 1, pp. e111–e117, 2012

0360-3016/$ - see front matter

ELSEVIER

doi:10.1016/j.ijrobp.2011.01.029

CLINICAL INVESTIGATION **Education and Training**

NATIONAL MEDICAL CARE SYSTEM MAY IMPEDE FOSTERING OF TRUE SPECIALIZATION OF RADIATION ONCOLOGISTS: STUDY BASED ON STRUCTURE SURVEY IN JAPAN

Hodaka Numasaki, Ph.D.,* Hitoshi Shibuya, M.D.,† Masamichi Nishio, M.D.,‡ Hiroshi Ikeda, M.D.,§ Kenji Sekiguchi, M.D.,‖ Norihiko Kamikonya, M.D.,¶ Masahiko Koizumi, M.D.,# Masao Tago, M.D.,** Yutaka Ando, M.D.,†† Nobuhiro Tsukamoto, M.D.,‡‡ Atsuro Terahara, M.D.,§§ Katsumasa Nakamura, M.D.,‖‖ Michihide Mitsumori, M.D.,¶¶ Tetsuo Nishimura, M.D.,## Masato Hareyama, M.D.,*** Teruki Teshima, M.D.*, and Japanese Society of Therapeutic Radiology and Oncology Database Committee

*Department of Medical Physics and Engineering, Osaka University Graduate School of Medicine, Suita, Osaka, Japan; †Department of Radiology, Tokyo Medical and Dental University, Tokyo, Japan; ‡Department of Radiology, National Hospital Organization Hokkaido Cancer Center, Sapporo, Hokkaido, Japan; §Department of Radiology, Sakai Municipal Hospital, Sakai, Osaka, Japan; ‖Department of Radiation Oncology, St. Luke's International Hospital, Tokyo, Japan; ¶Department of Radiology, Hyogo College of Medicine, Nishinomiya, Hyogo, Japan; #Oncology Center, Osaka University Hospital, Suita, Osaka, Japan; **Department of Radiology, Teikyo University School of Medicine University Hospital, Mizonokuchi, Kawasaki, Kanagawa, Japan; ††Department of Medical Informatics, Heavy Ion Medical Center, National Institute of Radiological Sciences, Chiba, Japan; ‡‡Department of Radiation Oncology, Saitama Medical University International Medical Center, Saitama, Japan; §§Department of Radiology, Toho University Omori Medical Center, Tokyo, Japan; ‖‖Department of Radiology, Kyushu University Hospital at Beppu, Oita, Japan; ¶¶Department of Radiation Oncology and Image-applied Therapy, Graduate School of Medicine Kyoto University, Kyoto, Japan; ##Division of Radiation Oncology, Shizuoka Cancer Center, Shizuoka, Japan; and ***Department of Radiology, Sapporo Medical University, Hokkaido, Japan

Purpose: To evaluate the actual work environment of radiation oncologists (ROs) in Japan in terms of working pattern, patient load, and quality of cancer care based on the relative time spent on patient care.

Methods and Materials: In 2008, the Japanese Society of Therapeutic Radiology and Oncology produced a questionnaire for a national structure survey of radiation oncology in 2007. Data for full-time ROs were crosschecked with data for part-time ROs by using their identification data. Data of 954 ROs were analyzed. The relative practice index for patients was calculated as the relative value of care time per patient on the basis of Japanese Blue Book guidelines (200 patients per RO).

Results: The working patterns of RO varied widely among facility categories. ROs working mainly at university hospitals treated 189.2 patients per year on average, with those working in university hospitals and their affiliated facilities treating 249.1 and those working in university hospitals only treating 144.0 patients per year on average. The corresponding data were 256.6 for cancer centers and 176.6 for other facilities. Geographically, the mean annual number of patients per RO per quarter was significantly associated with population size, varying from 143.1 to 203.4 ($p < 0.0001$). There were also significant differences in the average practice index for patients by ROs working mainly in university hospitals between those in main and affiliated facilities (1.07 vs 0.71: $p < 0.0001$).

Conclusions: ROs working in university hospitals and their affiliated facilities treated more patients than the other ROs. In terms of patient care time only, the quality of cancer care in affiliated facilities might be worse than that in university hospitals. Under the current national medical system, working patterns of ROs of academic facilities in Japan appear to be problematic for fostering true specialization of radiation oncologists. © 2012 Elsevier Inc.

Structure survey, Working pattern, Patient load, Quality of cancer care, Medical care system.

Reprint requests to: Teruki Teshima, M.D., Department of Medical Physics and Engineering, Osaka University Graduate School of Medicine 1-7, Yamadaoka, Suita, Osaka, 565-0871, Japan. Tel: +81-6-6879-2570; Fax: +81-6-6879-2570. E-mail: teshima@sahs.med.osaka-u.ac.jp

Supported by the Japanese Society of Therapeutic Radiology and Oncology (JASTRO) and Grants-in-Aid for Cancer Research (No. 18-4, 20S-5, and H19-3rd Term Cancer Control General-038) from the Ministry of Health, Labor and Welfare of Japan and by a Grant-in-Aid for Scientific Research from the Japan Society for the Promotion of Sciences (No. 19390320 and 20591495).

Conflict of interest: none

Acknowledgments—We thank all radiation oncologists throughout Japan who participated in this survey for their efforts in providing us with valuable information to make this study possible.

Received Oct 15, 2010, and in revised form Dec 8, 2010. Accepted for publication Jan 12, 2011.

INTRODUCTION

The medical care systems of the United States and Japan are very different, which influences the personnel cost of medical staff. In radiation oncology, too, there is thus a major difference in personnel distribution between the United States and Japan. Most radiotherapy facilities in the United States are supported by full-time radiation oncologists (ROs), whereas the majority of radiotherapy facilities in Japan still rely on part-time ROs. Radiotherapy facilities with less than one full-time equivalent (FTE) RO on their staff still account for 56% nationwide (1). The Cancer Control Act was implemented in Japan in 2007 in response to patients' urgent petitions to the government (2). This act strongly advocates the promotion of radiotherapy (RT) and an increase in the number of ROs and medical physicists. However, a shortage of ROs still remains a major concern in Japan and will remain so for the foreseeable future.

The Japanese Society of Therapeutic Radiology and Oncology (JASTRO) has conducted national structure surveys of RT facilities in Japan every 2 years since 1990 (1, 3). The structure of radiation oncology in Japan has improved in terms of equipment and its functions in response to the increasing number of cancer patients who require RT.

In this study, we used the data of the JASTRO structure survey of 2007 to evaluate the actual work environment of radiation oncologists in Japan in terms of working pattern, patient load, and the quality of cancer care based on the relative time spent on patient care.

MATERIALS AND METHODS

Between March and December 2008, JASTRO carried out a national structure survey of radiation oncology in the form of a questionnaire in 2007 (1). The questionnaire consisted of questions about the number of treatment machines and modality by type, the number of personnel by job category, the number of patients by type, and the site. The response rate was 721 of 765 (94.2%) from all actual RT facilities in Japan.

Table 1 shows the overview of radiation oncology in Japan. University hospitals accounted for 15.8% of all RT facilities and had 40.0% of the total full-time ROs and treated 29.5% of all patients. The corresponding data were 4.0%, 7.8%, and 10.2% for cancer centers, and 80.2%, 52.2%, and 60.3% for other RT hospitals, respectively. "Full-time/part-time" indicates the employment pattern of RO. In Japan, even full-time ROs must work part-time in smaller facilities such as other RT hospitals. We considered these numbers to be inappropriate for accurate assessment of personnel. For this survey, we therefore collected FTE (40 h/week for radiation oncology services only) data depending on hours worked in clinical RT of each RO. For example, if an RO works 3 days at a university hospital and 2 days at an affiliated hospital each week, FTE of the RO at the university hospital is 0.6 and at an affiliated hospital it is 0.4. The FTE of a facility that has three ROs with 0.8, 0.4, and 0.6 is calculated as 1.8 in total.

This survey collected the work situation data of a total of 1,007 full-time ROs and 534 part-time ROs. The data of full-time ROs were crosschecked with those of part-time ROs by using their identification data. Table 2 shows the result of crosschecking between data of full-time ROs and data of part-time ROs. In this study, data of 954 ROs were analyzed. Table 3 shows an overview of the analyzed data. In ROs working mainly in university hospitals, there are two ROs who worked at a maximum of six facilities (main facilities and five affiliated facilities) SAS 8.02 (SAS Institute Inc., Cary, NC) (4) was used for the statistical analysis, and the statistical significance was tested by means of the Student's *t*-test or analysis of variance.

The Japanese Blue Book guidelines (5, 6) for structure of radiation oncology in Japan based on Patterns of Care Study (PCS) data were used as the standard for comparison with the results of this study. PCS in Japan have been used since 1996 and have disclosed significant differences in the quality of RT by the type of facilities and their caseloads (7, 8). The standard guidelines for annual patient load per FTE RO have been set at 200 (warning level 300).

To evaluate quality of cancer care provided by ROs, the relative practice index for patients was calculated by the following expression.

$$\frac{\sum_{k=1}^{n} f_k}{\sum_{k=1}^{n} a_k} \times 200$$

in which n is the number of facilities that the RO works in ($n = 1, 2, 3, \ldots, k$), f_k is the FTE of the RO in facility k, and a_k is the annual number of patients per RO in facility k

Calculation method of coefficient "200:"

1) Number of weeks per year = (365–15)/7 = 50 weeks
   ※ Japan has 15 national holidays a year
2) 1.0 FTE = 40 h/week
3) Annual working hours of FTE 1.0 = 50 × 40 h = 2,000 h
4) Relative practice index for patients was normalized using the Blue Book guideline of 200 patients/FTE RO. For this guideline, care time per patient was set at 10 hours (2,000 h/200 patients).
5) Coefficient was 200 (2000/10).

RESULTS

Working patterns

Figure 1 shows working patterns of ROs working mainly in (a) university hospitals, (b) cancer centers, and (c) other

Table 1. Categorization of radiotherapy facilities in Japan

Facility category	Number of facilities	New patients	Total patients (new + repeat)	Full-time ROs		Part-time ROs	
				n	FTE	*n*	FTE
University hospital	114	50,351	60,555	403	293.0	70	21.6
Cancer center	29	16,794	20,968	78	73.7	14	2.5
Other radiotherapy hospital	578	103,084	123,564	526	351.8	450	83.7
Total	721	170,229	205,087	1,007	718.5	534	107.8

Abbreviations: RO = radiation oncologist; FTE = full-time equivalent (40 hours per week for radiation oncology services only).

Table 2. Connection between full-time and part-time RO data

Data of full-time ROs	
Total number	1,007
Number of full-time ROs excluded from this analysis*	53
Number of full-time ROs analyzed	954
Breakdown	
Number of ROs who worked as full-time staff at main facilities and as part-time staff at affiliated facilities	199
Number of ROs who conducted only radiotherapy-related work as full-time staff at individual facilities (FTE of the RO was 1.0)	275
Number of ROs who conducted radiotherapy-related and other work as full-time staff at individual facilities (FTE of the RO was less than 1.0)	480
Data of part-time ROs including duplicate ROs	
Total number	534
Number of ROs who worked as full-time staff at main facilities and as part-time staff at affiliated facilities (number of part-time ROs analyzed)	280
Number of ROs who worked as only part-time staff at the facilities (Number of part-time ROs excluded from this analysis)	254

Abbreviations: RO = radiation oncologist; FTE = full-time equivalent (40 hours per week for radiation oncology service only).
* Data of full-time ROs who worked at facilities with few patients were excluded, as were duplicated data of full-time ROs.

RT hospitals. The percentages of white parts in Figures 1 (a-c) were 17.4%, 5.0%, and 32.0%.

In university hospitals, the mean FTE RO for main facilities was 0.73 and for affiliated facilities it was 0.10. The corresponding figures were 0.94 and 0.01 for cancer centers, and 0.67 and 0.01 for other RT hospitals. For university hospitals, the ratio of ROs working only in main facilities was 16.4%, and the corresponding figures for cancer centers and other RT hospitals were 79.5% and 31.7%, respectively. The ratio of ROs working mainly in university hospitals and part-time in affiliated facilities was 44.5%. The corresponding data were 6.5% of ROs working primarily in cancer centers and 7.5% of ROs working mainly in other RT hospitals.

Patient loads

Figure 2(a) shows the patient load per RO working mainly in university hospitals, cancer centers, and other RT hospitals. Of ROs working primarily in university hospitals, 40.1% treated more than 200 patients per year. The corresponding ratios were 74.4% of ROs working primarily in cancer centers and 36.5% of those working mainly in other RT hospitals. The average number of patients treated by ROs working primarily in university hospitals was 189.2, with the corresponding figures being 256.6 patients in cancer centers and 176.6 in other RT hospitals. Figure 2(b) shows the patient load per RO working primarily in university hospitals. Of ROs working in university hospitals and affiliated facilities, 65.9% treated more than 200 patients per year, and the percentage was 19.3% of ROs working only in university hospitals. The former treated an average of 249.1 patients and the latter 144.0 patients per year.

The geographic patterns

Figure 3 shows the geographic distribution for 47 prefectures of the mean annual number of patients (new plus repeat) per RO arranged in order of increasing population by all prefectures in Japan (9). The average annual number of patients per RO per quarter ranged from 143.1 to 203.4, with significant differences among quarters ($p < 0.0001$). Figure 4 shows the top 10 prefectures with ROs who treated more than 200 patients per year in descending order: Tokyo, Osaka, Kanagawa, Hokkaido, Chiba, Aichi, Fukuoka, Hyogo, Miyagi, and Hiroshima.

Relative practice index for patients of ROs

Figure 5(a) shows the average relative practice index for patients of ROs in university hospitals and affiliated facilities (ROs working mainly in university hospitals). The average practice index of RO for patients was 1.07 at university hospitals and 0.71 at affiliated facilities for a statistically significant difference ($p < 0.0001$). Figure 5(b) shows the average relative practice index for patients of ROs working only in university hospitals, only in cancer centers, and only in other RT hospitals. The respective indices for the three categories were 1.26, 1.02, and 1.01. There were significant differences in the indices between university hospitals and cancer centers ($p = 0.0278$) and between university hospitals and other RT hospitals ($p < 0.0001$). The difference between cancer

Table 3. Overview of analyzed data

Main facility category	Number of full-time ROs working at main facilities	Number of part-time ROs working at affiliated facilities					
		First*	Second*	Third*	Fourth*	Fifth*	Subtotal
University hospital	372	160	59	14	4	2	239
Cancer center	78	5	0	0	0	0	5
Other radiotherapy hospital	504	34	2	0	0	0	36
Total	954	199	61	14	4	2	280

Abbreviation: RO = radiation oncologist.
* First: first affiliated facilities; second: second affiliated facilities; third: third affiliated facilities; fourth: fourth affiliated facilities; fifth: fifth affiliated facilities.

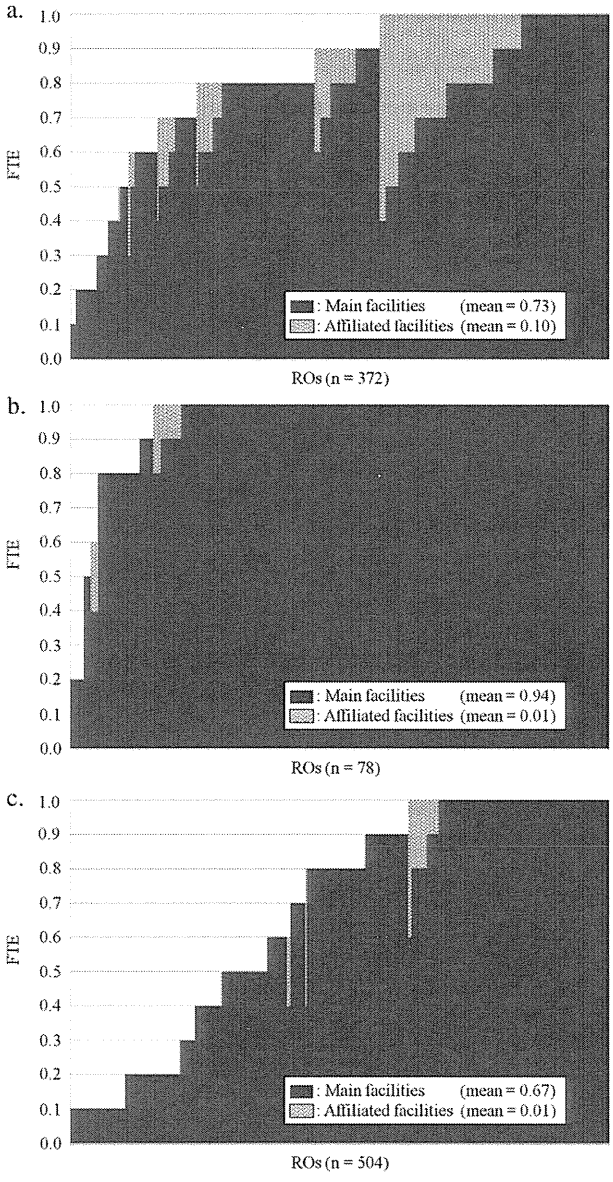

Fig. 1. Working patterns of ROs working mainly at (a) university hospitals, (b) cancer centers, and (c) other radiotherapy hospitals. Distribution of FTE ratio between main and affiliated facilities on each RO. Horizontal axis represents ROs in ascending order of own total FTE. *Abbreviations:* RO = radiation oncologist; FTE = full-time equivalent (40 hours per week for radiation oncology services only).

centers and other RT hospitals was not significant ($p = 0.9459$).

DISCUSSION

In the United States, most RT facilities are supported by full-time ROs, with an FTE of 1.0 for most ROs working at their own facilities. In Japan, on the other hand, more than a half of the facilities still rely on part-time ROs. The main reason of this discrepancy is a shortage of ROs. Between 2005 and 2007, the increase in the number of cancer

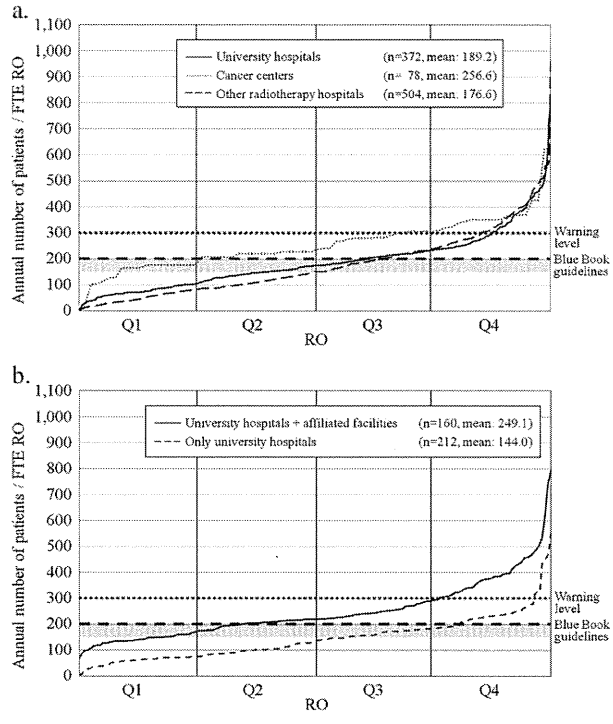

Fig. 2. Distribution of annual patient load/RO. (a) RO working mainly in university hospitals, cancer centers, and other radiotherapy hospitals. (b) RO working mainly in university hospitals. Horizontal axis represents ROs in ascending order of annual numbers of patients/RO. Q1: 0–25%, Q2: 26–50%, Q3: 51–75%, Q4: 76–100%. *Abbreviations:* RO = radiation oncologist; FTE = full-time equivalent (40 hours per week for radiation oncology services only).

patients requiring RT (7.3%) was higher than that in the number of FTE ROs (6.7%) (1). To make up for the shortage of ROs, most ROs in university hospitals must work part-time at affiliated hospitals, as is evident from the date shown in Figure 1. White parts of Figure 1 (a: 17.4%, b: 5.0% c: 32.0%) represent three types of data: (a) FTE data of ROs who were not provided in the survey questionnaire; (b) FTE data of part-time ROs whose identification data could not connect to those of full-time ROs; (c) FTE data of ROs working in nonradiation oncology services. In this survey, the data of type (a) and (b) were missing data and the data of type (c) were not collected. In other RT hospitals, the FTE of most ROs working in their own facilities is low and these ROs do not work part-time at other hospitals. There are two reasons for this. First, diagnosticians partly provide RT as ROs in their own hospitals and, second, other specialists (such as brain surgeons using gamma knife) partly function as ROs to provide RT. Because those facilities have few cancer patients, their patient load is less than that of university hospitals and cancer centers. These findings are evident from Figure 2(a). There was a major difference in the working patterns of ROs between university hospitals and cancer centers. FTE at their own facilities of most ROs working in university hospitals is less than 1.0, whereas that of most ROs working in cancer centers is 1.0,

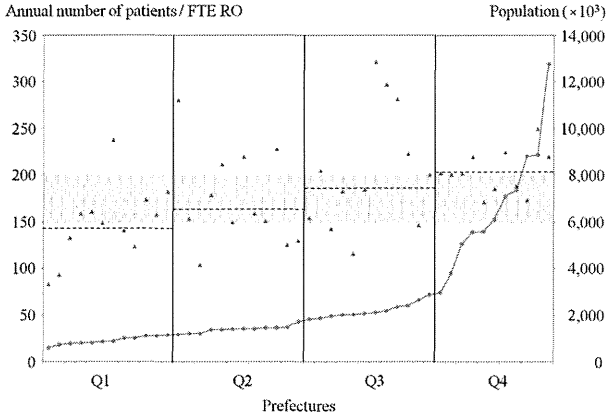

Fig. 3. Geographic distribution for 47 prefectures of annual number of patients (new plus repeat) per RO in ascending order of prefectural population. Q1: 0–25%; Q2: 26–50%; Q3: 51–75%; Q4: 76–100%. Triangles represent average annual number of patients per RO for each prefecture. Blue circles show prefectural population. Horizontal broken lines indicate the average annual number of patients per RO per quarter. The shaded area represents the Japanese Blue Book guideline (150–200 patients per RO). *Abbreviations:* RO = radiation oncologist; FTE = full-time equivalent (40 hours per week for radiation oncology services only).

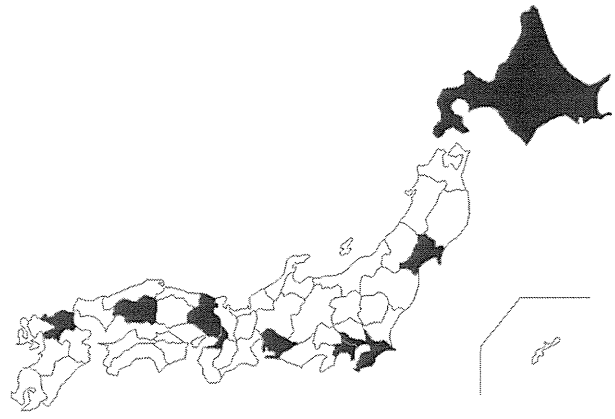

Fig. 4. The top 10 prefectures with ROs who treated more than 200 patients in descending order: Tokyo, Osaka, Kanagawa, Hokkaido, Chiba, Aichi, Fukuoka, Hyogo, Miyagi, and Hiroshima. *Abbreviation:* RO = radiation oncologist.

the same as in the United States and European countries. The shortage of ROs is not the only reason for the problems facing Japan. The pay system of ROs is another important reason. The salary of ROs in Japan is low because specialist medical fees for ROs are not covered by the Japanese healthcare insurance system. Moreover, the salary of ROs in university hospitals is lower than in other types of facilities, so that most of these ROs must work part-time at affiliated hospitals to earn a living. One advantage of this system, however, is that advanced technology is introduced sooner and faster in affiliated hospitals.

The geographic patterns demonstrated significant differences in the patient load among prefectures, ranging from 83.2 to 321.4 patients per RO. There were more ROs in metropolitan than other areas. However, the number of ROs who had more than 200 patients (new plus repeat) was strongly associated with population (correlation coefficient: 0.94), so that the number of ROs in metropolitan area remained insufficient.

Gomi *et al.* reported that the survival rate of patients treated in academic RT facilities (university hospitals and cancer centers) was better than that of those treated in nonacademic RT facilities in Japan (10). In this study, the proportion of facilities with part-time ROs in nonacademic RT facilities group was higher than that in academic RT facilities group. Part-time ROs have less care time per patient because they had a limit to working hours. On the basis of the presented evidence, the relative practice index for patients of ROs was calculated as one way to valuate quality of cancer care in this study. Concerning ROs working primarily in university hospitals, the average relative practice index for patients in affiliated facilities was less than that in main facilities (university hospitals). Teshima *et al.* reported that academic RT facilities (university hospitals and cancer centers) had better equipments and manpower than nonacademic RT facilities (1). Therefore, ROs at large-scale university hospitals might be given sufficient support because large-scale university hospitals tend to have state-of-the-art equipment, practice leading-edge medical treatment techniques, and employ enough medical staff members. On the other hand, ROs of most affiliated facilities could provide only minimal cancer care because these facilities

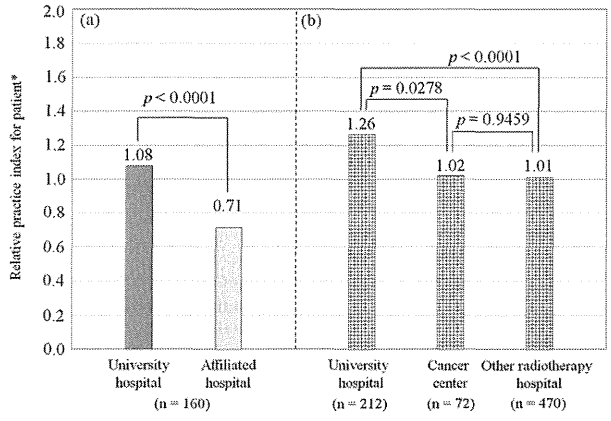

Fig. 5. Relative practice index for patients of ROs. (a) Relative practice index for patients in university hospitals and affiliated hospitals (targeted ROs were working mainly in university hospitals and part-time in affiliated hospitals). (b) Relative practice index for patients in university hospitals, cancer centers, and other radiotherapy hospitals (targeted ROs were working only in university hospitals or cancer centers only or only in other radiotherapy hospitals). *The formula used for calculating relative practice index for patients is: $\frac{\sum_{k=1}^{n} f_k}{\sum_{k=1}^{n} a_k} \times 200$ n: number of facilities that the RO works in (n = 1, 2, 3, …, k). f_k : FTE of the RO in facility k a_k : annual number of patients per RO in facility k. *Abbreviations:* RO = radiation oncologist; FTE = full-time equivalent (40 hours per week for radiation oncology services only).

tend to lack sufficient equipment and medical staff. Moreover, commuting between large-scale university hospitals and affiliated facilities resulted in a waste of time and in tiredness. Therefore, the quality of cancer care in affiliated facilities was worse than that in large-scale university hospitals. Although the annual number of patients per RO in cancer centers was higher than that in university hospitals and other RT hospitals, the average relative practice index for patients of ROs working only in cancer centers was lower than that for patients of ROs working only in university hospitals and equal to that for patients of ROs working only in other RT hospitals. It can thus be concluded that ROs in cancer centers worked efficiently.

The utilization rate of RT for new cancer patients in Japan is much lower than that in European countries and the United States. Because there are enough RT facilities distributed nationwide in Japan, an increase in the number of Ros would likely result in a spectacular improvement in the utilization rate of RT for new cancer patients. To increase the number of ROs, it is necessary to improve the work environment and conditions for radiation oncology in medical care facilities. One, feasible suggestion is for RT facilities to set up a new department of radiation oncology, so that the position of RO will be established at every such facility and the status of radiation oncology will improve as a result. In addition, the Cancer Control Act was approved in 2006 and the Basic Plan to Promote Cancer Control Program was approved by the Japanese Cabinet in 2007 to promote RT and education for ROs as well as other RT staff members. For the implementation of this law and plan, the availability of basic data of RO working conditions is essential. As a start, an education program called "Cancer Professional Training Plan" was started in April 2008 with the support of the Ministry of Education, Culture, Sports, Science and Technology.

Quality of cancer care was evaluated in this study with the aid of the relative practice index for patients. However, data concerning the processes and outcomes for cancer care using RT should be used for a more accurate evaluation of cancer care. In the United States, the National Cancer Data Base has been collecting data for cancer care. The data of National Cancer Data Base are useful for quality evaluation of cancer care (11, 12). Furthermore, PCS has been performed every 4 or 5 years since 1973 for a survey of the structure, processes, and outcomes of radiation oncology facilities (13). As PCS evolved into Quality Research in Radiation Oncology, periodic assessments of radiation oncology have been conducted for evaluation of practice quality on a national basis. In Japan, the structure, processes and outcomes for cancer care using RT have been investigated by PCS every 4 years (7, 8). The Japanese PCS has evaluated the quality of cancer care with RT and provided evidence of the disparity in quality of RT among facilities (14–18). However, these data are insufficient because PCS is a two-stage cluster sampling survey. We have recently established a database system based on available radiation oncology data and the collection of cancer care data by means of this system is now in preparation.

This study based on the JASTRO structure survey has indicated that the current national medical care system may impede fostering of true specialization of radiation oncologists in Japan because it is suffering from systemic fatigue. Although private hospitals make much money by receiving fee-for-service reimbursement, public hospitals face major deficit problems. It is therefore necessary to redistribute the burden of medical costs. On the other hand, the Japanese medical care system is beneficial for patients and national finances. Japan has had a universal health insurance system since 1961. Even though the per-capita medical costs in Japan were less than half of those in the United States and the medical costs in relation to the gross domestic product in Japan were about half of those in the United States as of 2007 (19), the outcome of cancer treatment in Japan is the same or better than in the United States. It is therefore very important to collect at regular intervals detailed information about all cancer care facilities for evaluation of quality of care and medical care systems for cancer. In Japan, the JASTRO structure survey has collected structural data of radiation oncology. Furthermore, a database system for the collection of data regarding the processes and outcomes for cancer care has recently been established in Japan as well as an information infrastructure for evaluation of the quality of care in radiation oncology.

In conclusion, our survey found that ROs working in university hospitals and their affiliated facilities treated more patients than did other ROs. In terms of patient care time only, the quality of cancer care in affiliated facilities might be worse than that in university hospitals. Under the current national insurance system, working patterns of ROs in academic facilities in Japan tend to impede the fostering of true specialization of radiation oncologists.

REFERENCES

1. Teshima T, Numasaki H, Shibuya H, *et al.* Japanese structure survey of radiation oncology in 2007 based on institutional stratification of Patterns of Care Study. *Int J Radiat Oncol Biol Phys* 2010;78:1483–1493.
2. Maeda M. A review of cancer control strategy in Japan [in Japanese]. *J Natl Inst Public Health* 2008;57:304–307.
3. Teshima T, Numasaki H, Shibuya H, *et al.* Japanese structure survey of radiation oncology in 2005 based on institutional stratification of Patterns of Care Study. *Int J Radiat Oncol Biol Phys* 2008;2:144–152.
4. SAS Institute Inc. SAS User's Guide: Statistics. Cary, NC: SAS Institute Inc.; 1985.
5. Japanese PCS Working Group. Radiation oncology in multidisciplinary cancer therapy -Basic structure requirement for quality assurance of radiotherapy based on Patterns of Care Study in Japan. Ministry of Health, Labor and Welfare Cancer Research Grant Planned Research Study 14-6, 2005.
6. Japanese PCS Working Group. Radiation oncology in multidisciplinary cancer therapy -Basic structure requirement for quality assurance of radiotherapy based on Patterns of Care Study in

Japan. Ministry of Health, Labor and Welfare Cancer Research Grant Planned Research Study 18-4, 2010.
7. Tanisada K, Teshima T, Ohno Y, *et al.* Patterns of Care Study quantitative evaluation of the quality of radiotherapy in Japan. *Cancer* 2002;95:164–171.
8. Teshima T, Japanese PCS working group. Patterns of Care Study in Japan. *Jpn J Clin Oncol* 2005;35:497–506.
9. Ministry of Internal Affairs and Communications, Statistics Bureau, Director-General for Policy Planning (Statistical Standards) & Statistical Research and Training Institute. Current population estimates as of October 1, 2007. Available from: www.stat.go.jp/english/data/jinsui/2007np/index.htm (accessed August 31, 2010).
10. Gomi K, Oguchi M, Hirokawa Y, *et al.* Process and preliminary outcome of a patterns-of-care study of esophageal cancer in Japan: Patients treated with surgery and radiotherapy. *Int J Radiat Oncol Biol Phys* 2003;56:813–822.
11. National Cancer Data Base. Available from: www.facs.org/cancer/ncdb/index.html (accessed June 30, 2010).
12. Bilimoria KY, Stewart AK, Winchester DP, *et al.* The National Cancer Data Base: A powerful initiative to improve cancer care in the United States. *Ann Surg Oncol* 2008;15:683–690.
13. Wilson JF, Owen JB. Quality research in radiation oncology: A self-improvement initiative 30 years ahead of its time? *J Am Coll Radiol* 2005;2:1001–1007.
14. Yamauchi C, Mitsumori M, Sai H, *et al.* Patterns of care study of breast-conserving therapy in Japan: Comparison of the treatment process between 1995–1997 and 1999–2001 surveys. *Jpn J Clin Oncol* 2007;38:26–30.
15. Toita T, Kodaira T, Uno T, *et al.* Patterns of radiotherapy practice for patients with cervical cancer (1999–2001): Patterns of Care Study in Japan. *Int J Radiat Oncol Biol Phys* 2008;70:788–794.
16. Kenjo M, Uno T, Numasaki H, *et al.* Radiation therapy for esophageal cancer in Japan: Results of the Patterns of Care Study 1999–2001. *Int J Radiat Oncol Biol Phys* 2009;75:357–363.
17. Uno T, Sumi M, Numasaki H, *et al.* Changes in patterns of care for limited-stage small cell lung cancer: Results of the 99-01 Patterns of Care Study—A nationwide survey in Japan. *Int J Radiat Oncol Biol Phys* 2008;71:414–419.
18. Ogawa K, Nakamura K, Onishi H, *et al.* Japanese Patterns of Care Study Working Subgroup of Prostate cancer. External beam radiotherapy for clinically localized hormone-refractory prostate cancer: Clinical significance of nadir prostate-specific antigen value within 12 months. *Int J Radiat Oncol Biol Phys* 2009;74:759–765.
19. OECD Health Data 2010. Paris: Organisation for Economic Co-Operation and Development; 2010.

Journal of Radiation Research, 2013, 54, 561–568
doi: 10.1093/jrr/rrs122 Advance Access Publication 13 December 2012

Guidelines for respiratory motion management in radiation therapy

Yukinori MATSUO[1], Hiroshi ONISHI[2], Keiichi NAKAGAWA[3], Mitsuhiro NAKAMURA[1,*], Takaki ARIJI[4], Yu KUMAZAKI[5], Munefumi SHIMBO[6], Naoki TOHYAMA[7], Teiji NISHIO[8], Masahiko OKUMURA[9], Hiroki SHIRATO[10] and Masahiro HIRAOKA[1]

[1]Department of Radiation Oncology and Image-applied Therapy, Kyoto University Graduate School of Medicine, 54 Shogoin-Kawaharacho, Sakyo-ku, Kyoto-shi, Kyoto 606-8507, Japan
[2]Department of Radiology, School of Medicine, University of Yamanashi, 1110 Shimokato, Chuo-shi, Yamanashi 409-3898, Japan
[3]Department of Radiology, The University of Tokyo, 7-3-1 Hongo, Bunkyo-ku, Tokyo 113-8655, Japan
[4]Department of Radiology, National Cancer Center Hospital East, 6-5-1 Kashiwanoha, Kashiwa-shi, Chiba 277–8577, Japan
[5]Department of Radiation Oncology, Saitama Medical University International Medical Center, 1397–1 Yamane, Hidaka-shi, Saitama 350-1298, Japan
[6]Department of Radiology, Saitama Medical Center, 1981 Kamoda, Kawagoe-shi, Saitama 350–8550, Japan
[7]Division of Radiation Oncology, Chiba Cancer Center, 666-2 Nitona-cho, Chuo-ku, Chiba 260-8717, Japan
[8]Particle Therapy Division, Research Center for Innovative Oncology, National Cancer Center, 6-5-1 Kashiwanoha, Kashiwa-shi, Chiba 277-8577, Japan
[9]Department of Central Radiological Service, Kinki University School of Medicine, 377-2 Ohno-higashi, Osakasayama-shi, Osaka, 589-8511, Japan
[10]Department of Radiation Medicine, Hokkaido University Graduate School of Medicine, Kita-15, Nishi-5, Kita-ku, Sapporo-shi, Hokkaido 060-8638, Japan
*Corresponding author. Department of Radiation Oncology and Image-applied Therapy, Kyoto University Graduate School of Medicine, 54 Shogoin-Kawaharacho, Sakyo-ku, Kyoto-shi, Kyoto 606-8507, Japan. Tel: +81-75-751-3762; Fax: +81-75-771-9749; Email: m_nkmr@kuhp.kyoto-u.ac.jp

(Received 21 September 2012; accepted 21 November 2012)

Respiratory motion management (RMM) systems in external and stereotactic radiotherapies have been developed in the past two decades. Japanese medical service fee regulations introduced reimbursement for RMM from April 2012. Based on thorough discussions among the four academic societies concerned, these Guidelines have been developed to enable staff (radiation oncologists, radiological technologists, medical physicists, radiotherapy quality managers, radiation oncology nurses, and others) to apply RMM to radiation therapy for tumors subject to respiratory motion, safely and appropriately.

Keywords: radiotherapy; guideline; respiratory motion; respiratory motion management

INTRODUCTION

External radiotherapy synchronized with the respiration-gating signal was developed three decades ago [1]. Since then, respiratory motion management (RMM) systems in external and stereotactic radiotherapies have been investigated and improved [2, 3]. In Japan, changes to medical service fee regulations in April 2012 introduced fees for RMM in external and stereotactic radiotherapies. These techniques have been accepted as effective radiation therapies for tumors that are subject to respiratory motion, as techniques that allow precise targeting of the tumors with prescribed radiation dosages, while reducing the dosage of irradiation to unaffected tissue surrounding tumors.

Using RMM makes it possible to reduce the irradiated area and lower the incidence of adverse effects in principle. However, it is necessary to bear in mind that, without great care, this kind of treatment poses risks that may lead to unintended treatment results.

Based on extensive discussions among the four academic societies concerned (the Japan Conformal External Beam Radiotherapy Group, the Japanese Society for Therapeutic Radiology and Oncology, the Japan Society of Medical Physics, and the Japanese Society of Radiological Technology), these Guidelines have been developed to enable staff (radiation oncologists, radiological technologists, medical physicists, radiotherapy quality managers, radiation oncology nurses, and others) involved in this kind of treatment to apply RMM to radiation therapy for tumors subject to respiratory motion, safely and appropriately.

Definitions of RMMs

RMMs

RMMs must meet the following requirements:

(i) The treatment detailed here may only be applied when the length of respiratory tumor motion exceeds 10 mm without RMM being implemented. When the three-dimensional length of motion exceeds 10 mm, the evaluation must be that 'the length of respiratory-induced motion exceeds 10 mm'. For example, if the lengths of motion in the craniocaudal, right-left, and dorsoventral directions are 9 mm, 4 mm, and 4 mm, respectively, the three-dimensional length is calculated as $\sqrt{9^2 + 4^2 + 4^2} = 10.6$ mm, so fulfilling the requirements of these Guidelines. The length of the respiratory-induced tumor motion must be measured under free, unforced breathing, and irregularities in the respiration due to hiccups, coughs, sneezes and deep respiration are to be excluded. Some institutions stipulate in the medical fee regulatory standards that treatment of 'tumors whose length of respiratory motion is 10 mm or longer' must be categorized as Tokkei-Shinryo (therapies covered by special schedules). However, the Guidelines detailed here assume that RMM is applicable to tumors where the length of respiratory motion exceeds 10 mm.

(ii) In the treatment plans, it must be ascertained and recorded that the expansion of area of irradiation required to compensate for respiratory motion can be reduced to ≤ 5 mm in any direction, three-dimensionally. In regulations for medical treatment fees and institutional standards, two different expressions are used: 'expansion of field of irradiation required due to respiratory motion', and 'expansion of area of irradiation required to compensate for respiratory motion'. However, the present guidelines use only the expression: 'expansion of area of irradiation required to compensate for respiratory motion'. 'Expansion of area of irradiation required to compensate for respiratory motion' applies to both the length of the respiration-induced tumor motion, as well as to the uncertainties related to RMM, and is equivalent to a part of the internal margin defined in ICRU (International Commission on Radiation Units and Measurements) Report 62 [4]. The three-dimensional direction refers to six directions: the cranio, caudal, right, left, dorso, and ventral directions, and the expansion of the irradiated area necessary in each direction must be 5 mm or less. If the expansion of area of irradiation required in order to compensate for respiratory motion is 5 mm or less in any one direction, then, where the irradiated area does not contract when compared with areas where RMM is not performed, it cannot be regarded as effective RMM.

(iii) At every instance of irradiation treatment, it is necessary to ascertain and record that the tumor is included in the irradiated area determined in (ii), immediately prior to and during the irradiation. 'Immediately prior to the irradiation' refers to the time from placing the patient on the treatment table in the room where the irradiation will take place until the start of the first beam of irradiation of the treatment. 'During the irradiation' refers to the time during which each treatment beam takes place. 'A tumor is included in the irradiated area' means that a tumor is included in the planning target volume (PTV), three-dimensionally. However, 2D confirmation is acceptable during the irradiation.

When it is difficult to directly verify that the tumor is included in the irradiated area, it is acceptable to confirm this based on a marker in the body that represents the tumor positions, such as a marker in the vicinity of the tumor. In such cases, it is assumed that the method of predicting tumor positions based on the particular marker has been verified.

It is necessary to verify that a tumor is included in the irradiated area immediately prior to the irradiation. Furthermore, it is recommended to verify this state, the inclusion of the tumor in the irradiated area, during the irradiation. (According to the description in the document for medical treatment fees, this verification should be performed immediately prior to the irradiation OR during the irradiation; however, these Guidelines specify the performance of the verification immediately prior to the irradiation as indispensable.)